

Autonomous Platooning of General Connected Vehicles Using Bayesian Receding Horizon Control

Gilchrist Johnson
VICTOR Lab
 University of Virginia
 Charlottesville, VA, USA
 email: gilchristjohnson@virginia.edu

Tomonari Furukawa
VICTOR Lab
 University of Virginia
 Charlottesville, VA, USA
 email: tomonari@virginia.edu

B. Brian Park
Link Lab
 University of Virginia
 Charlottesville, VA, USA
 email: bp6v@virginia.edu

Abstract—This paper focuses on futuristic connected vehicles and presents a strategy for autonomous platooning of general connected vehicles including low-speed utility vehicles, which drive over various terrains, not limited to roads. In such general environments, the goal of a following vehicle is to keep following its preceding vehicle with minimum distance and without collision. Since the vehicles are connected, the following vehicle in the proposed strategy receives the controls of its immediate preceding vehicle through communications and predicts a future pose of the preceding vehicle in a receding horizon. Further, the prediction incorporates the inertial motion and is probabilistically executed in the framework of Recursive Bayesian Estimation by fusing the two distributions predicted by a particle filter through Gaussian approximation. The performance of the proposed strategy was investigated using simulated golf carts with a drive-by-wire system. The proposed strategy has been found to improve the accuracy of the conventional following by 30.4%.

Index Terms—autonomous following; connected vehicles; recursive bayesian estimation; receding horizon control.

I. INTRODUCTION

The last two decades have seen the dramatic advancement of vehicle autonomy including autonomous platooning, which allows a sequence of vehicles to drive autonomously. While the leader vehicle may also be automated, the first interest of autonomous platooning results in autonomously navigating a follower vehicle such that it keeps a targeted distance from its preceding vehicle during the entire navigation. Autonomous following has become the primary concern of autonomous platooning.

Past work on autonomous vehicles can be primarily studied in two applications. With society's interest, recent efforts have been most exerted on autonomous driving where vehicles are expected to be driven with a minimum or target distance to minimize traffic congestion while avoiding collision [1]. Since roads are structured well having planar surfaces with various marks and signs, such as lanes, the majority of the work was conducted on the detection and localization of such objects and autonomous following in the reduced free space [2]. Because vehicles on public roads are not connected to each other, follower vehicles determine their final control actions based on what they can observe using their sensors.

The second application is often known in the name of multi-robot cooperation. Formation control is a synchronous approach where all the robots including the leader are controlled to maintain the pre-designed formation [3][4]. This is not the

approach of interest in this paper since the paper is concerned with the autonomous control of a following vehicle only. The other popular approach is the leader-follower approach where each of the follower robots sequentially and independently determines its path after the path of the leader is given [5]–[7], which is along with the interest of this paper and has been widely studied. Some early work planned a path to pass through waypoints whereas trajectories specifying states in full-led follower robots subject to dynamic behavior more accurately [8]. Extended work includes that of [9] which developed a collision avoidance strategy for environments with obstacles that do not allow the maintenance of the pre-designed formation. Communication between the leader robot and a follower robot was proposed by [10] to transmit the follower's path computed by the leader after the leader redesigned its path for obstacle avoidance. The technique works well if the leader robot is autonomous. However, the full autonomy of the leader robot in the real world is still unrealistic, so autonomous following should be developed for manually operated leader vehicles.

This paper presents a strategy for autonomous following of general connected vehicles including low-speed utility vehicles. The proposed technique does not rely on traffic marks and signs to drive over various terrains and enhances its autonomous following capability by using vehicle connectivity; the following vehicle receives the controls of its immediate preceding vehicle through communications and predicts a future pose of the preceding vehicle in a receding horizon. Further, the prediction incorporates the inertial motion and is probabilistically executed in the framework of Recursive Bayesian Estimation (RBE) by fusing the two distributions predicted by a Particle Filter (PF) through Gaussian approximation.

The paper is organized as follows. The next section describes the mathematical foundation of the leader vehicle estimation problem and two conventional techniques to achieve autonomous following. Section III presents the technique which is proposed to enhance autonomous following leveraging vehicle connection. Experimental studies are conducted in Section IV, and conclusions and future work are summarized in the final section.

II. RECURSIVE BAYESIAN ESTIMATION

A. Leader and Follower Vehicle Models

Consider a leader vehicle l with its unknown global state given by $\mathbf{x}^l \in \mathcal{X}^l$, the motion of which is generically modeled by

$$\mathbf{x}_k^l = \mathbf{f}^l(\mathbf{x}_{k-1}^l, \mathbf{w}_k^l), \quad (1)$$

where \mathbf{w}_k^l is a motion noise. This leader vehicle is observed by an autonomous follower vehicle f , the global state of which is evolved with the motion model

$$\mathbf{x}_k^f = \mathbf{f}^f(\mathbf{x}_{k-1}^f, \mathbf{u}_k^f, \mathbf{w}_k^f), \quad (2)$$

where $\mathbf{x}_k^f \in \mathcal{X}^f$ and $\mathbf{u}_k^f \in \mathcal{U}^f$ represent the state and control input of the follower vehicle, respectively, and $\mathbf{w}_k^f \in \mathcal{W}^f$ is the motion noise of the follower vehicle.

The follower vehicle will be equipped with various sensors including those for self-localization and those for observation of targets of interest and environments. To focus on autonomous following, the pose of the follower vehicle is assumed to be known exactly, so only the model of the sensor for leader vehicle localization is thus formulated:

$${}^f\mathbf{z}_k^l = {}^f\mathbf{h}^l(\mathbf{x}^l, \mathbf{x}_k^f, {}^f\mathbf{v}_k^l) \quad (3)$$

where ${}^f\mathbf{z}_k^l$ is the observation of the leader vehicle by the sensor on the follower vehicle, and ${}^f\mathbf{v}_k^l$ represents the observation noise [13].

B. Recursive Bayesian Estimation

In the context of autonomous following, the RBE generically estimates belief on the leader vehicle in the global coordinate frame. This is done by representing the belief in terms of a Probability Density Function (PDF) and recursively updating it through prediction and correction. Let us consider a generic scenario where a sequence of observations of the leader vehicle by the follower vehicle is given by ${}^f\tilde{\mathbf{z}}_{1:k}^l \equiv \{{}^f\tilde{\mathbf{z}}_{\kappa}^l | \forall \kappa \in \{1, \dots, k\}\}$. Note here that (\cdot) represents an instance of variable (\cdot) . Given the initial belief $p(\mathbf{x}_0^l)$ and the sequence of observations ${}^f\tilde{\mathbf{z}}_{1:k}^l$, the lead vehicle belief at time step k , $p(\mathbf{x}_k^l | {}^f\tilde{\mathbf{z}}_{1:k}^l, \tilde{\mathbf{x}}_{1:k}^f)$, is updated as follows:

Prediction: Computes the follower vehicle belief at k $p(\mathbf{x}_k^l | {}^f\tilde{\mathbf{z}}_{1:k-1}^l, \tilde{\mathbf{x}}_{1:k-1}^f)$ from the belief updated at $k-1$ $p(\mathbf{x}_{k-1}^l | {}^f\tilde{\mathbf{z}}_{1:k-1}^l, \tilde{\mathbf{x}}_{1:k-1}^f)$. The prediction is carried out by Chapman-Kolmogorov equation:

$$p(\mathbf{x}_k^l | {}^f\tilde{\mathbf{z}}_{1:k-1}^l, \tilde{\mathbf{x}}_{1:k-1}^f) = \int_{\mathcal{X}^l} p(\mathbf{x}_k^l | \mathbf{x}_{k-1}^l) p(\mathbf{x}_{k-1}^l | {}^f\tilde{\mathbf{z}}_{1:k-1}^l, \tilde{\mathbf{x}}_{1:k-1}^f) d\mathbf{x}_{k-1}^l, \quad (4)$$

where $p(\mathbf{x}_k^l | \mathbf{x}_{k-1}^l)$ is a Markov motion model defined by (1).

Correction: Computes the robot and target belief $p(\mathbf{x}_k^l | {}^s\tilde{\mathbf{z}}_{1:k}^l, \tilde{\mathbf{x}}_{1:k}^f)$ given the predicted belief $p(\mathbf{x}_k^l | {}^f\tilde{\mathbf{z}}_{1:k-1}^l, \tilde{\mathbf{x}}_{1:k-1}^f)$ and the new observation ${}^f\tilde{\mathbf{z}}_k^l$ at the new state $\tilde{\mathbf{x}}_k^f$. The equation is derived by applying formulas

for marginal distribution and conditional independence and given by

$$p(\mathbf{x}_k^l | {}^f\tilde{\mathbf{z}}_{1:k}^l, \tilde{\mathbf{x}}_{1:k}^f) = \frac{l(\mathbf{x}_k^l | {}^f\tilde{\mathbf{z}}_k^l, \tilde{\mathbf{x}}_k^f) p(\mathbf{x}_k^l | {}^f\tilde{\mathbf{z}}_{1:k-1}^l, \tilde{\mathbf{x}}_{1:k-1}^f)}{\int_{\mathcal{X}^l} l(\mathbf{x}_k^l | {}^f\tilde{\mathbf{z}}_k^l, \tilde{\mathbf{x}}_k^f) p(\mathbf{x}_k^l | {}^f\tilde{\mathbf{z}}_{1:k-1}^l, \tilde{\mathbf{x}}_{1:k-1}^f) d\mathbf{x}_k^l}, \quad (5)$$

where $l(\mathbf{x}_k^l | {}^f\tilde{\mathbf{z}}_k^l, \tilde{\mathbf{x}}_k^f)$ represents the likelihood of \mathbf{x}_k^l given observation ${}^f\tilde{\mathbf{z}}_k^l$.

There are two approaches that have been commonly used for the autonomous control of the follower vehicle. The inexpensive approach is observation based and determines the next control of the follower vehicle \mathbf{u}_{k+1}^f using the latest observation ${}^f\tilde{\mathbf{z}}_k^l$ and the current state $\tilde{\mathbf{x}}_k^f$; the control \mathbf{u}_{k+1}^f is found such that the belief resembles the observation likelihood:

$$J(l(\mathbf{x}_k^l | {}^f\tilde{\mathbf{z}}_k^l, \tilde{\mathbf{x}}_k^f)) = \left\| \mathbf{g}\left(l(\mathbf{x}_k^l | {}^f\tilde{\mathbf{z}}_k^l, \tilde{\mathbf{x}}_k^f)\right) - (\mathbf{x}_{k+1}^f + \mathbf{d}_k) \right\|_2 \rightarrow \min_{\mathbf{u}_{k+1}^f} \quad (6)$$

where

$$\mathbf{x}_{k+1}^f = \mathbf{f}^f(\tilde{\mathbf{x}}_k^f, \mathbf{u}_{k+1}^f, \tilde{\mathbf{w}}_{k+1}^f), \quad (7)$$

$\mathbf{g}(\cdot)$ returns the centroid of the likelihood, and \mathbf{d}_k is the desired gap of the follower vehicle to the leader vehicle. $\|\cdot\|$ is an L^2 norm.

The more intelligent approach identifies a sequence of n_c controls, $\mathbf{u}_{k+1:k+n_c}^f$, by predicting the belief recursively up to the $(k+n_c)$ -th time step in the framework of receding horizon control (RHC):

$$J(p(\mathbf{x}_{k+n_c}^l | {}^f\tilde{\mathbf{z}}_{1:k}^l, \tilde{\mathbf{x}}_{1:k}^f)) = \left\| \mathbf{g}\left(p(\mathbf{x}_{k+n_c}^l | {}^f\tilde{\mathbf{z}}_{1:k}^l, \tilde{\mathbf{x}}_{1:k}^f)\right) - (\tilde{\mathbf{x}}_{k+n_c}^f + \mathbf{d}_k) \right\|_2 \rightarrow \min_{\mathbf{u}_{k+1:k+n_c}^f} \quad (8)$$

where

$$p(\mathbf{x}_{k+\kappa}^l | {}^f\tilde{\mathbf{z}}_{1:k}^l, \tilde{\mathbf{x}}_{1:k}^f) = \int_{\mathcal{X}^l} p(\mathbf{x}_{k+\kappa}^l | \mathbf{x}_{k+\kappa-1}^l) p(\mathbf{x}_{k+\kappa-1}^l | {}^f\tilde{\mathbf{z}}_{1:k}^l, \tilde{\mathbf{x}}_{1:k}^f) d\mathbf{x}_{k+\kappa-1}^l, \quad (9a)$$

$$\mathbf{x}_{k+\kappa}^f = \mathbf{f}^f(\tilde{\mathbf{x}}_{k+\kappa-1}^f, \mathbf{u}_{k+\kappa}^f, \tilde{\mathbf{w}}_{k+\kappa}^f) \quad (9b) \\ \forall \kappa \in \{1, \dots, n_c\}$$

It is to be noted that (8) may be represented with an integral payoff instead of the terminal payoff.

Both approaches work well if the leader vehicle has a predictable motion and moves within the range the follower vehicle can track. However, the motion of the leader vehicle is, precisely, given not by (1) but by

$$\mathbf{x}_k^l = \mathbf{f}^l(\mathbf{x}_{k-1}^l, \mathbf{u}_k^l, \mathbf{w}_k^l), \quad (10)$$

where the control of the leader vehicle, \mathbf{u}_k^l , significantly affects its motion in addition to the motion noise \mathbf{w}_k^l . If the intention

of the leader vehicle, $\mathbf{u}_{k+1:k+n_c}^l$, is beyond the expectation, the follower vehicle may not be able to track the leader vehicle successfully. The number of steps to look ahead n_c , as a consequence, cannot be large, which results in unstable controls.

III. AUTONOMOUS PLATOONING

A. Overview

Figure 1 illustrates the proposed technique for autonomous platooning. The technique is built on conventional methods but incorporates novel leader intention prediction, which was originally proposed by the authors for robotic escorting [11][12]. The following vehicle estimates the current pose of the leader vehicle \mathbf{x}_k^l and predicts its future pose $\mathbf{x}_{k+n_p}^{l,\alpha}$ from the current pose using the RBE as the conventional following does. Here, the superscript α indicates the conventional following whereas n_p indicates the number of steps to look ahead by the proposed technique. However, the future pose of the leader vehicle in the proposed technique is additionally predicted as $\mathbf{x}_{k+n_p}^{l,\beta}$ using the current leader vehicle data transmitted through connection to the follower vehicle including the steering angle and the vehicle speed, which cannot be observed well. Here, the superscript β indicates the prediction using the leader vehicle's control. The proposed technique then fuses the two predictions and determines future controls $\mathbf{u}_{k+1:k+n_p}^f$ using the RHC. Prediction using the vehicle control data is an additional effective source for follower control because the current control is often the intention of the leader vehicle in a longer time horizon. The number of steps to look ahead by the proposed technique, n_p , is thus larger than that of the conventional technique n_c , and the prediction by the proposed technique is also expected to be more accurate. The follower vehicle, thus, can potentially achieve more smooth and successful platooning even in noisier environments.

B. Prediction Using Particle Filter

The steering angle of the leader vehicle cannot be observed from the follower vehicle whereas the speed of the leader vehicle cannot be accurately measured from the follower vehicle due to the dynamic relative motion. Since it receives the precise steering angle and vehicle speed through connection, $\tilde{\mathbf{u}}_k^l$, the follower vehicle can identify what the leader vehicle intends to do. Let the intended control that may be used up to the time step $k + n_p$ be $\mathbf{u}_{k \rightarrow n_p}^l \sim \mathcal{N}(\tilde{\mathbf{u}}_k^l, \Sigma_k^{l,u})$. Using the PF, the pose of the leader vehicle can be then predicted by leveraging the intention as

$$\mathbf{x}_{k+\kappa,i}^\beta = \mathbf{f}^\beta \left(\mathbf{x}_{k+\kappa-1}^{\beta,i}, \mathbf{u}_{k \rightarrow n_p}^{\beta,i}, \mathbf{w}_k^{\beta,i} \right), \quad \forall \kappa \in [1, \dots, n_p], \forall i \in [1, \dots, N], \quad (11)$$

where $\mathbf{w}_k^{\beta,i} \sim \mathcal{N}(\bar{\mathbf{w}}_k^\alpha, \Sigma_k^{\beta,w})$, and N is the number of particles.

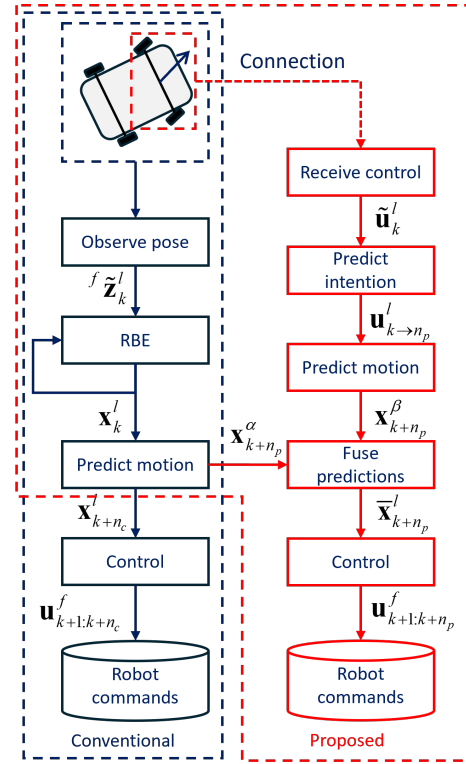


Figure 1. Conventional platooning vs. proposed platooning.

The pose can also be predicted using the motion model without the control as

$$\mathbf{x}_{k+\kappa+1}^{\alpha,i} = \mathbf{f}^\alpha \left(\mathbf{x}_{k+\kappa}^{\alpha,i}, \mathbf{w}_k^{\alpha,i} \right), \quad \forall \kappa \in [1, \dots, n_p], \forall i \in [1, \dots, N], \quad (12)$$

where $\mathbf{w}_k^{\alpha,i} \sim \mathcal{N}(\bar{\mathbf{w}}_k^\alpha, \Sigma_k^{\alpha,w})$. Note that the PF is used in the proposed technique because the motion model is non-Gaussian; the particles of both predictions will be spread in a non-Gaussian manner in the state space due to the nonlinearity of the motion models. Clearly, prediction with control is more accurate if the current control lasts long in the future whereas prediction with the current pose and without control is more accurate if the current control is given transitionally. The level of confidence of the predictions is determined by $\Sigma_k^{\alpha,w}$, $\Sigma_k^{\beta,w}$ and $\Sigma_k^{l,u}$. While $\Sigma_k^{\alpha,w}$ in the model without control modeling is much larger than $\Sigma_k^{\beta,w}$, the control uncertainty $\Sigma_k^{l,u}$, which is added to \mathbf{f}^β , becomes the factor to determine which prediction is more certain.

C. Receding Horizon Control Based on the Hybrid Prediction

Once they have been spread over the state space, the two sets of particles must be fused to ultimately determine the control action. The proposed approach uniquely approximates each distribution as a Gaussian distribution. This approximation is valid since random noise dominates the distribution over time.

By definition, the mean and the covariance of each distribution is calculated as

$$\bar{\mathbf{x}}_{k+n_p}^{(\cdot)} = \frac{1}{N} \sum_{i=1}^N \mathbf{x}_{k+n_p}^{(\cdot),i} \quad (13a)$$

$$\Sigma_{k+n_p}^{(\cdot)} = \frac{1}{N} \sum_{i=1}^N \left(\mathbf{x}_{k+n_p}^{(\cdot),i} - \bar{\mathbf{x}}_{k+n_p}^{(\cdot)} \right) \left(\mathbf{x}_{k+n_p}^{(\cdot),i} - \bar{\mathbf{x}}_{k+n_p}^{(\cdot)} \right)^\top \quad (13b)$$

where (\cdot) is prediction without control α or prediction with control β , and \top represents the transpose of the matrix. The mean of the probability distribution combining the two distributions can be then derived through the multiplication:

$$\bar{\mathbf{x}}_{k+n_p}^l = \frac{\Sigma_{k+n_p}^\beta}{\Sigma_{k+n_p}^\alpha + \Sigma_{k+n_p}^\beta} \bar{\mathbf{x}}_{k+n_p}^\alpha + \frac{\Sigma_{k+n_p}^\alpha}{\Sigma_{k+n_p}^\alpha + \Sigma_{k+n_p}^\beta} \bar{\mathbf{x}}_{k+n_p}^\beta. \quad (14)$$

Now that the target pose of the leader vehicle in the n_p step lookaheads is identified, the RHC determines a sequence of control actions of the follower vehicle by minimizing the objective function:

$$J \left(\bar{\mathbf{x}}_{k+n_p}^l \right) = \left\| \bar{\mathbf{x}}_{k+n_p}^l - \left(\mathbf{x}_{k+n_p}^f + \mathbf{d}_k \right) \right\|_2 \rightarrow \min_{\mathbf{u}_{k+1:k+n_p}^f} \quad (15)$$

where

$$\mathbf{x}_{k+\kappa}^f = \mathbf{f}^f \left(\mathbf{x}_{k+\kappa-1}^f, \mathbf{u}_{k+\kappa}^f, \tilde{\mathbf{w}}_{k+\kappa}^f \right), \quad \forall \kappa \in \{1, \dots, n_p\}. \quad (16)$$

IV. EXPERIMENTAL RESULTS

A. Experimental Settings

The proposed technique was evaluated using two golf carts in a simulated environment, which are available to the authors for real-world demonstration in the future. Each cart has a full set of components for autonomous platooning including a communication module for vehicle connection, a stereo camera for relative pose measurement, a GPS and IMU for global positioning, and a drive-by-wire system for computer-controlled actuation. The simulated carts used the same components. Figure 2(a) shows the real cart whereas their simulated version is shown in Figure 2(b). In order to validate the efficacy of the proposed platooning technique over conventional techniques, the two conventional techniques described in Section II were also used for autonomous platooning. One was observation based with no prediction and connection, and the other was with prediction but without connection. Since the aim of the experimental analysis is the proof-of-concept, the motion models of the leader cart and the follower cart were for the two-dimensional space and given by

$$x_k^{(\cdot)} = v_k^{(\cdot)} \cos \theta_k^{(\cdot)} \quad (17a)$$

$$y_k^{(\cdot)} = v_k^{(\cdot)} \sin \theta_k^{(\cdot)} \quad (17b)$$

$$\theta_k^{(\cdot)} = \frac{v_k^{(\cdot)}}{L} \tan \gamma_k^{(\cdot)}, \quad (17c)$$



(a) Golf cart.



(b) Simulated golf cart.

Figure 2. Physical vs. simulated systems.

where $\mathbf{x}_k^{(\cdot)} = [x_k^{(\cdot)}, y_k^{(\cdot)}, \theta_k^{(\cdot)}]^\top$ is the set of state variables, and $\mathbf{u}_k^{(\cdot)} = [v_k^{(\cdot)}, \gamma_k^{(\cdot)}]^\top$ is the set of control variables. (\cdot) is l or f . For the leader cart model with no control information, the motion model with the controls of the average observed speed \bar{v}_k^l and 0 steering angle was used since it is valid to assume that the cart moves straight with the current orientation. The relative difference $\mathbf{d}_k = [d_{x,k}, d_{y,k}, d_{\theta,k}]^\top$ places the follower cart behind the leader cart in the same orientation:

$$d_{x,k} = d \cos \theta_k^l \quad (18a)$$

$$d_{y,k} = d \sin \theta_k^l \quad (18b)$$

$$d_{\theta,k} = 0, \quad (18c)$$

where d is the targeted distance. In the numerical simulation, the leader cart was programmed to drive a winding path since the proposed technique is effective when the cart is turning. Table I lists the parameters used in the experiment.

TABLE I
PARAMETERS FOR EXPERIMENT

Parameter	Value
L	1.2 [m]
\bar{v}_k^l	8.5 [m/s]
d	4 [m]
$\Sigma_k^{l,u}$	[0.1, 0, 0, 0.087] [m,m,m]
$\tilde{\mathbf{w}}_k^\alpha$	[0.5, 0.5] [m,m]
$\Sigma_k^{\alpha,w}$	[0.05, 0, 0, 0.017] [m,m,m,m]
$\tilde{\mathbf{w}}_k^\beta$	[0.5, 0.5] [m,m]
$\Sigma_k^{\beta,w}$	[0.5, 0, 0, 0.087] [m,m,m,m]
N	1000

B. Results

Figure 3 shows the results of the proposed platooning technique compared to those of the two conventional techniques. Figure 3(a) first shows the paths of the follower cart by the proposed and the conventional techniques in addition to those of the leader cart and the ideal follower cart. The path of the ideal follower cart $\mathbf{x}_k^{\text{ideal}}$, given that of the leader cart \mathbf{x}_k^l is given by

$$\mathbf{x}_k^{\text{ideal}} = \mathbf{x}_k^l - \mathbf{d}_k. \quad (19)$$

The closer the path to that of the ideal follower cart, the better the path. It is seen that the path of the proposed technique is significantly better than that of the conventional techniques. The observation based technique with neither prediction nor connection is shown to have the worst path partly because the control of the leader cart is not observable and partly because this limited observation is the only source of information to determine the control of the follower cart; if the observation is noisy, the control fluctuates according to the noisy observation and thus becomes inaccurate. The prediction based technique with no connection performs better but is still inefficient when compared to the proposed technique. This is due to the lack of information on the control of the leader cart, which makes the prediction of the future pose of the leader cart more accurate. Figure 3(b) shows the error in the orientation of the follower cart with respect to the ideal orientation. The superiority of the proposed technique to the conventional techniques can also be seen in this result since the configuration of the orientation with the proposed technique captures that of the leader cart most.

Figure 3(c) lastly shows the positional error. The positional error is defined by

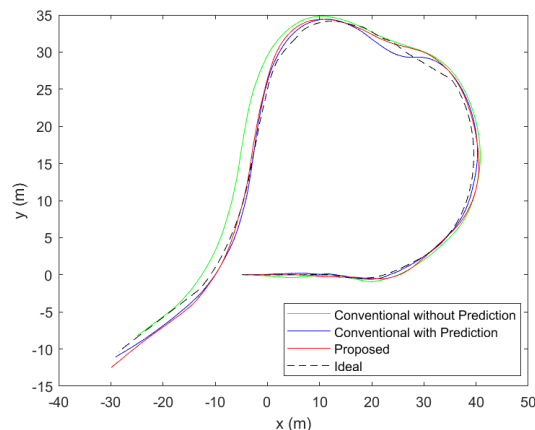
$$E_k^{(\cdot)} = \left\| \mathbf{x}_k^{\text{ideal}} - \bar{\mathbf{x}}_k^f \right\|_2 \quad (20)$$

It is seen that the proposed technique yields the minimum positional errors constantly, which is the result of the prediction using information through vehicle connectivity. The mean positional error of the proposed technique is 3.7% whereas that of the conventional observation and prediction techniques are 8.0% and 5.3%, respectively. The error of the proposed technique is particularly small around 10 seconds when the cart is turning maximally. This is because the technique used information on the turning. The result conclusively shows that the proposed technique has improved the accuracy of the conventional techniques by 30.4%.

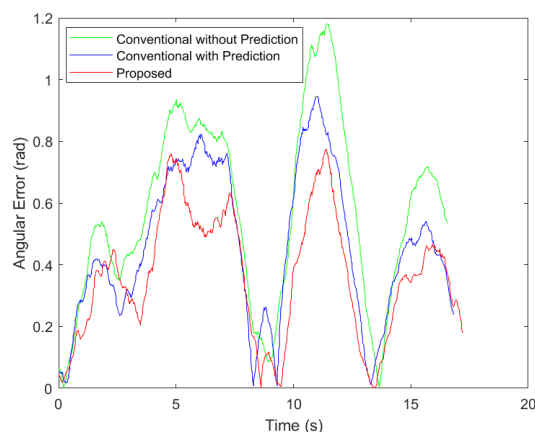
V. CONCLUSION AND FUTURE WORK

This paper has presented a strategy for autonomous following of general connected vehicles. In the proposed strategy, the following vehicle receives the controls of its immediate preceding vehicle through communications and predicts a future pose of the preceding vehicle using the PF and the Gaussian fusion. The autonomous control of the follower vehicle is finally determined through the RHC. The performance of the proposed strategy was investigated using simulated golf carts with a drive-by-wire system. The results show that the proposed strategy improved the accuracy by 30.4%, and it was particularly effective when the leader cart was turning sharply.

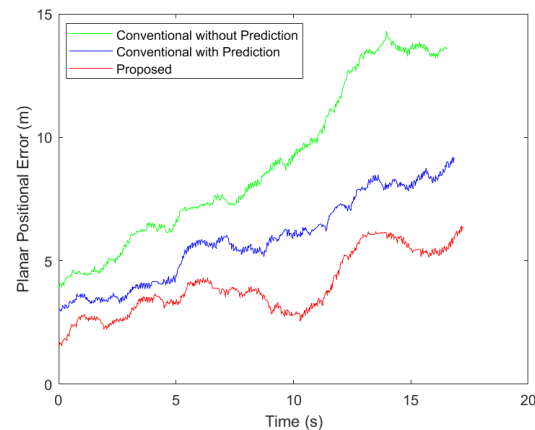
The paper shows only the preliminary results and much future work is possible. Ongoing work includes experimental validation using the real golf carts, modeling of uncertainties and the effect, and the reduction of communication delay. Communication delay weakens the effect of the proposed technique, so minimizing it is an essential task to complete.



(a) Vehicle path.



(b) Angular root mean squared error.



(c) Planar position error.

Figure 3. Simulation results.

ACKNOWLEDGMENT

This work is sponsored by the US Office of Naval Research (N00014-23-1-2572). The authors would like to express their sincere gratitude to Dr. Tom McKenna at the Office of Naval Research for his invaluable support and advice. Special thanks

also go to Mr. Dean Conte at Mitre Corporation who developed the base technique of this paper during his graduate study.

REFERENCES

- [1] D. Milakis, B. van Arem, and B. van Wee, "Policy and society related implications of automated driving: a review of literature and directions for future research," *J. Intel. Transp. Sys.*, vol. 21, no. 4, pp. 324-348, 2017.
- [2] A. AM. Assidiq, O. O. Khalifa, M. R. Islam, and S. Khan, "Real time lane detection for autonomous vehicles," *Int. Conf. Comp. Comm. Eng.*, Kuala Lumpur, pp. 82-88, 2008.
- [3] A. Loria, J. Dasedemir, and N. A. Jarquin, "Leader-follower formation and tracking control of mobile robots along straight paths," *IEEE Trans. Cont. Sys. Tech.*, vol. 24, no. 2, pp. 727-732, 2016.
- [4] M. M. Alam, M. Y. Arafat, S. Mah, and J. Shen, "Topology control algorithms in multi-unmanned aerial vehicle networks: an extensive survey," *J. Network. Comp. Appl.*, vol. 207, 103476, 2022.
- [5] T. Fukao, H. Nakagawa, and N. Adachi, "Adaptive tracking control of a nonholonomic mobile robot," *IEEE Trans. Rob. Auto.*, vol. 16, no. 5, pp. 609-615, 2000.
- [6] B. Madhevan, and M. Sreekumar, "Tracking algorithm using leader follower approach for multi robots," *Proc. Eng.*, vol. 64, pp. 1426-1435, 2013.
- [7] M. Bujarbaruah, Y. R. Sturz, C. Holda, K. H. Johansson, and F. Borrelli, "Learning environment constraints in collaborative robotics: a decentralized leader-follower approach," 2012 IEEE/RSJ Int. Conf. Intel. Rob. Sys., Prague, 2021.
- [8] A. Gasparetto, P. Boscariol, A. Lanzutti, and R. Vidoni, "Path planning and trajectory planning algorithms: a general overview," *Motion and Operation Planning of Robotic Systems*, pp. 3-27, 2015.
- [9] T. Bhavana, M. Nithya, and M. Rajesh, "Leader-follower co-ordination of multiple robots with obstacle avoidance," 2017 Int. Conf. Smart. Tech. Smart Nation, August 2017.
- [10] X. Wu, S. Wang, and M. Xing, "Observer-based leader-following formation control for multi-robot with obstacle avoidance," *IEEE Access*, vol. 7, pp. 14791-14798, 2018.
- [11] D. Conte and T. Furukawa, "Autonomous robotic escort incorporating motion prediction and human intention," 2021 IEEE Int. Conf. Rob. Auto., Xi'an, 2021.
- [12] D. Conte and T. Furukawa, "Autonomous Bayesian escorting of a human integrating intention and obstacle avoidance," *J. Field Rob.*, vol. 39, pp. 679-693, 2022.
- [13] T. Furukawa, F. Bougault, B. Lavis, and H. F. Durrant-Whyte, "Recursive Bayesian search-and-tracking using coordinated UAVs for lost targets," 2006 Int. Conf. Rob. Auto., pp. 2521-2526, 2006